Accepted manuscript doi:
10.1680/jwama.19.00074

Accepted manuscript doi:
10.1680/jwama.19.00074

Submitted: 13 September 2019

Published online in 'accepted manuscript' format: 24 March 2020

Manuscript title: Experimental study on the mechanisms of flow and sediment transport in a vegetated channel

Authors: Geng Qu[1], Shunqi Pan[2], Chengwei Hu[1], Shiming Yao[1], Bing Ding[1], Geng Qu and Fang Liu[3]

Affiliations: [1]Laboratory of River Regulation and Flood Control of MWR, Changjiang River Scientific Research Institute, Wuhan, China; [2]School of Engineering, Cardiff University, the Parade, Cardiff, UK and [3]State Key Laboratory of Hydraulic Engineering Simulation and Safety, School of Civil Engineering, Tianjin University, Tianjin, China

Corresponding author: Geng Qu, Laboratory of River Regulation and Flood Control of MWR, Changjiang River Scientific Research Institute, Wuhan 430010, China.

E-mail: qugeng0516@163.com

Accepted manuscript doi:
10.1680/jwama.19.00074

Abstract

Laboratory experiments were conducted in a flume with 3 types of artificial flexible submerged and emergent vegetation. Detailed velocity and sediment concentration in the channel were measured. The results show that submerged and emergent vegetation generates a much greater resistance to flow, and significantly alters the vertical distributions of velocity, especially in the vegetated and downstream regions. In comparison with the non-vegetated case, the turbulence kinetic energy and Reynolds stresses in the vegetated and downstream regions are much higher, indicating strong flow turbulence and momentum exchange in these areas. The high turbulence also results in a nearly constant fine suspended sediment concentration in the water column for all cases, while the increased resistance causes the coarser suspended sediment concentration to decrease. In addition, the sediment retention by the vegetation with small height is insignificant, but for the canopy with large height, the significant sediment deposition is found at the upstream region of the vegetated region.

Keywords: sediment transport; turbulence characteristics; vegetation; velocity structure

Accepted manuscript doi:
10.1680/jwama.19.00074

1 Introduction

A river ecosystem is determined by the characteristics of both terrestrial and aquatic ecosystems. Vegetation, serving as an important element of the river ecosystem, is an important factor influencing the erosion process and development of rivers (Wang et al., 2014). For example, river erosion always occurs when bank vegetation is disturbed. Because of the benefits that vegetation provides for water quality, habitat, and bank stability, the ecological restoration of the disturbed river ecosystems has become very popular worldwide in recent years (Mars et al. 1999, Pollen and Simon 2005). Design of sustainable ecological restoration projects, such as restoring the physical form of the historical rivers and reestablishing their natural functions, requires the knowledge of how the existence of vegetation influences bank stability. This needs a better understanding of the complex interactions between flow, sediment in vegetated rivers (Weston, 2014; Fagherazzi et al., 2017).

Despite significant research in recent years, there are still many questions associated with the interactions among flow, sediment and vegetation from both ecological and engineering perspectives (Nepf, 2012a, 2012b). For the flow-vegetation interaction, the presence of vegetation can influence the velocity field in vicinity of the vegetation patches. Specifically, because of the influence of the vegetation, the flow in the vegetated rivers is always three-dimensional, which has an effect on the distribution of flow characteristic parameters, such as flow velocity, turbulence intensity, Reynolds stress, etc. Many studies focused on this topic (Ikeda & Kanazawa, 1996; Nepf 1999; Nepf &Vivoni, 2000; Nepf et al., 2007; Nepf & Ghisalberti 2008; Nezu & Onitsuka, 2001; Carollo et al. 2002; Wilson et al., 2003; Ghisalberti & Nepf 2002, 2004, 2006; Tang et al. 2007; Righetti, 2008; Okamoto & Nezu; 2010; Termini 2015, 2017). For example, Nepf (1999) developed a physically based model which can describe the impact of emergent vegetation on drag, turbulence and diffusion for flow and also cover the natural range of vegetation density and stem Reynolds' numbers. Carollo et al. (2002) performed an experimental study on the flow over flexible bottom vegetation and proposed a theoretical velocity profile with a new version of the Prandtl's mixing length method. Termini (2017) investigated the influence of vegetation on cross-sectional flow and bed shear distribution along a high-curvature bend and found that both of the directionality of turbulent structures and the curvature-induced flow pattern are altered by the vegetation.

The sediment-vegetation interaction is much more complex. Shi and Cao (2000) found that the vegetation could not only block the bed-load transport effectively but also intercepted the suspended sediment movement. However, the experimental study by Elliott (2000) showed that compared with non-vegetation case, the presence of vegetation can reduce the sedimentation rate and make sediment more easily suspended. Lu (2008) investigated the suspended sediment transport in the rigid vegetated channel and analysed the influence of the vegetation on the distribution of turbulence and sediment concentration. Jordanova and James (2003) established an empirical formula for the rate of bed-load transport in non-submerged

rigid vegetated channel using the analogy of the equation of bed-load transport rate in non-vegetated rivers and their experimental data. Recent work by Yang and Nepf (2018) indicated that existing sediment transport models based on time-averaged bed shear stress are not accurate for regions with vegetation because these models fail to incorporate the influence of vegetation-generated turbulence. They showed that bed load transport is correlated with measured near-bed turbulence, K_t. Based on this finding, they proposed a K_t-based sediment transport model, which takes into account the role of vegetation-generated turbulence. Furthermore, Yang and Nepf (2019) extended this result and showed that the bed load transport can be predicted just from U, the channel average velocity and ϕ, the vegetation volume fraction.

In general, most foregoing research focused the influence of one kind of vegetation on flow characteristics and sediment transport. However, there are many kinds of aquatic vegetation in river ecosystem. Few studies focused on both submerged and emergent vegetation. In addition, because of the limitations caused by sediment sample collections and measurement equipment, few studies focused on the characteristics of flow and sediment transport within upstream and downstream region in partly vegetated channel. From the aforementioned, the purpose of the present research is to gain some insight into the interactions among flow, sediment and vegetation. The analysis was conducted with the aid of experimental data collected in a straight flume with three types of representative submerged and emergent artificial flexible vegetation. Based on the experimental data, the mechanisms underlying the interaction between flow and sediment transport in the channel was investigated. It should be noted that although such an analysis was restricted to the experimental conditions investigated in this work, these results are expected to improve the understanding of the flow characteristics and sediment transport in the vegetated channel and lay a foundation for further research.

2 Experimental facility and conditions

The experiments were performed at the Hydraulics Laboratory in Changjiang River Scientific Research Institute (Wuhan, China) using a 28 m long, 0.5 m wide and 0.5 m deep glass flume with a bed slope S_0 adjustable in a range of 0‰-5‰ (Fig. 1). A thin plastic board was laid on the bottom of the flume for planting the artificial vegetation. Flow discharge and sediment into the flume were supplied by different pumps at the inlet, which generate fully developed turbulent flow and a constant sediment concentration for the measured section in the middle of the flume. A 4 m long test section was partially covered with artificial vegetation starting from 8 m downstream the inlet of the flume. The distance between two nearby vegetated elements in the longitudinal and transverse directions were 5cm.

The coordinate system used is as follows: the x-axis is aligned along the streamwise direction, with $x = 0$ located 8m upstream of the vegetated region. The upstream region is long enough, which allows the boundary layer to develop fully before the flow enters in vegetated region of eth flume; the y-axis is perpendicular to it with $y = 0$ at the centreline of the flume; the z-axis points vertically upward from the horizontal (x,y) plane. (see Fig. 2a).

Accepted manuscript doi:
10.1680/jwama.19.00074

The velocity measurements were performed with an Acoustic Doppler Velocimeter (ADV). For the measurements presented in this work, the sampling frequency was 25 Hz and the acquisition time was 30 s. From the measured data, the time-averaged velocity vector and the fluctuating velocity vector can be obtained. Both flow velocity and suspended sediment concentration measurements were performed at 3 cross-sections upstream of the vegetated section (S1-S3), 1 cross-section within the vegetated section (S4) and 6 cross-sections downstream of the vegetated section (S5-S10). The measurements were performed only at the one side of the flume, because the flows can be regarded as symmetric (see Fig. 2b). Velocity was measured at 40 points along the vertical direction. In addition, electromagnetic flowmeters and automatic water level meter were applied to ensure the accuracy of experimental data. Malvern Laser Particle Sizer Analysis System was also used when determining the sediment sizes from sediment samples.

To investigate the effect of the vegetation on the flow characteristics and sediment transport in a vegetated flume, three types of artificial flexible vegetation were used in this study (Fig. 3). All three types of artificial vegetation (P1, P2 and P3) were made of the same flexible plastic material with density of 1.35 g/cm^3 and elastic modulus of 0.03×10^5 Mpa. All plastic vegetation has foliage and its flexibility characteristics were closely similar to the live or natural plants commonly found in the riparian zone of rivers in China. The height of P1, P2 and P3 was 3 cm, 15 cm and 45 cm, respectively. Fig. 4 shows the accumulative areas (A_{ve}) of the plants with their height (h_{ve}). It is clear from Fig. 4 that for P1 and P2, the accumulative area of the plants increases approximately linearly against the height. For P3, the accumulative area increases slower in the stem part, and faster in the transition zone and above.

The experimental arrangements and key flow statistics were summarized in Table 1. The flow discharge to the flume is 30 L/s; U is the average velocity; S_s is water surface. The water depth at the outlet of the flume is 35 cm. In all experiments, the slope of the flume in each experimental case was adjusted in order to make the flow at the inlet section as uniform as possible. Before the experiments with vegetation were performed, one preliminary experiment without vegetation was carried out to obtained the reference flow and turbulence level in the test section. The results from the initial control experiments reveal that: (1) the distance from the inlet to the test section is sufficient for removing the inlet effect; (2) the sampling frequency is sufficiently high to obtain accurate velocity profiles and turbulence characteristics (Li et al. 2015); (3) the flow and turbulence distributions at the inlet section were uniform. Cases P1 and P2 were for the submerged flexible vegetation with P1 and P2 vegetation planted, respectively; Case P3 is for the emergent flexible with vegetation P3 planted. In order to maintain the uniform flow conditions as much as possible for all cases at the given discharge, the bed slope of the flume was adjusted for individually as detailed in Table 1. It can be seen that for Case P3, due to limitation of the maximum adjustment allowed for the bed slope, the surface slope in the vegetated section is steeper, so that only approximate uniform flow can be generated.

For sediment supply in the present experiments, plastic synthetic sand with the dry density of 670 kg/m^3 (Sun and Wei 2005) was supplied at the inlet of the channel with the rate of 5.0 g/s. Fig. 5 shows the grading curves of the artificial sediment used for all cases and they follow a similar composition with a median particle size (D_{50}) of 0.18 mm.

3 Results and discussion

In this section, the results of three dimensional velocities, shear stresses, turbulence kinetic energy, sediment concentration and transport rate will be discussed.

3.1 Longitudinal flow velocity in stream-wise direction

As described previously, ADVs were used in the experiments to measure 3D instantaneous velocities. In this and following sections, the time-averaged horizontal velocity components (longitudinal, transverse and vertical) were denoted by u, and v respectively, and w is the time-averaged vertical velocity. Their depth-averaged values were denoted as U, V and W, respectively. In order to better understand the effect of artificial vegetation on the flow characteristics along the stream-wise direction, the analysis was focused on the longitudinal velocity distributions in the flume. Fig. 6 shows the time-averaged longitudinal velocity (u) profiles normalized by the depth-averaged longitudinal velocity (U) at 10 locations in the stream-wise direction along the centreline (S1-1 to S10-1 as shown in Fig. 3). It can be seen from Fig. 6, the vertical distributions of the longitudinal flow velocity for all cases (P0, P1, P2, P3) in the far upstream region (S1-1 and S2-1) were very similar, following in general the logarithmic distribution. At S3-1, the vertical distributions of the longitudinal flow velocity diversify noticeably, which shows that the impact of the vegetation propagates from downstream, particularly in the lower part of the water column ($z/H < 0.2$). At S4-1, under the influence of the vegetation, their vertical distributions of the longitudinal velocity exhibit completely different patterns for the different types of vegetation. For Case P1, the short vegetation, the velocity is considerable reduced below the top level of the vegetation, and above the top, the distribution recovers to follow the logarithmic distribution (as a liner distribution at logarithmic scale), but the slope is much larger than that of the reference case (P0). For Case P2, it follows a similar trend as that of Case P1, with the reduced velocity below the top of the vegetation. Above the top of the vegetation, the velocity generally follows the logarithmic distribution, with even a steeper velocity gradient. In both cases, due to the significant increase of the resistance with the presence of vegetation near the channel floor, the flow is pushed toward the up layer of the water column, causing the considerable increase of the longitudinal velocity. However, for Case P3, the velocity profile is found very different, increasing in the lower part until its maximum at the level of the top stem, then decreasing duo to the foliage in the up part of this type of vegetation (P3). The velocity distribution near the surface becomes irregular. In general, the velocity can be characterised into three regions: a low part with increasing velocity; a middle part with decreasing velocity; and an upper part with irregular velocity. This phenomenon can be attributed to the distribution of the frontal area of canopy. For the submerged cases, the blades were mainly

distributed near the water surface, and in the lower water column only stems were distributed, which makes the frontal area of canopy reach maximum near the surface and decreased mean velocity upward near the water surface. With small frontal area in the middle water depth and near the bottom, larger velocity was occurred in these regions. At S5-1, which is located immediately after the vegetated region, it can be seen that a start of the velocity recovering process, which continues at the downstream locations from S6-1 to S9-1. At S9-1, the velocity distributions were mostly recovered except for P3, which is seen to be almost fully recovered at S10-1.

3.2 Longitudinal flow velocity in transverse direction

To examine the longitudinal flow velocity variation along the transverse direction, the measured velocities at 3 selected stream-wise locations were presented. Fig. 7 shows that the vertical distributions of the longitudinal velocity at 5 locations along the transverse direction (The distances were 0cm, 4cm, 8cm, 15cm, 21cm respectively from the centreline of the flume) at sections S1, S4 and S8. At section S1, the velocity distributions appeared to consistent despite some minor discrepancies. The effect of wall can be seen from those at S1-5. However, the distributions of the flow velocity at section S4 were clearly influenced, as seen for Cases P1 and P4, the influence for Case P2 is interestingly minimal. It is believed that the arrangement of vegetation planting and natural uncertainty could have affected the measurements. Similarly, at section S8, the downstream of the vegetated region, the velocity distributions diversify in the transverse direction, with particularly the effect of the flume wall. The distribution discrepancies were highly dependent on the shapes and planting patterns of the vegetation, as well as the interaction between flow and vegetation as the increase of resistance in all cases (Qu et al. 2015), which demonstrates a strong three-dimensionality of the flow. Nevertheless, the use of velocity measurements from the locations along the centreline will be largely representative without losing much of generality in the following sections.

3.3 Flow shear stress

As shown in Fig. 7, the different flow velocity distributions in the water column were revealed under different test conditions. In order to understand the shear stress distributions in the water column and impact of the vegetation, the velocity gradients were assessed. Fig. 8 shows the calculated the gradients of the longitudinal velocity from the time-averaged velocities at three positions: S1-1, S4-1 and S8-1. In the upstream region (S1-1), the flow velocity gradient of three Cases P1, P2 and P3 were basically similar to that of Case P0, with highest values at the location z/H= 0.05 approximately, and decreasing toward the water surface. The results indicate that the different types of vegetation have less influence on the flow velocity gradient in the far upstream region. In the vegetated region (S4-1), due to the influence of the vegetation, the flow velocity gradient changes significantly in different vertical zones. For submerged vegetation (Cases P1 and P2), the flow velocity gradient is significantly increased near the top of vegetation. Whilst for the emergent vegetation (Case P3), the flow velocity gradient is significantly increased near the height of 0.4z/H (the upper

edge of transition between stems and upper foliage). In the downstream region (S8-1), the influence on the flow pattern by the vegetation still exists. The impact is greatest for Case P3. Yet, the vertical distribution of the flow velocity gradient of Cases P1, P2 and P3 gradually approaches that of Case P0 along the stream-wise direction.

The analysis of the vertical distribution of flow velocity shows that 1) the vertical distribution of flow velocity for Case P0 complied with the logarithmic distribution. 2) For the submerged vegetation (Cases P1 and P2), taking into account the general flexibility of the vegetation and their lodging in the flow, the practical heights of them in the flow should be lower than their real heights. 3) For emergent vegetation (Case P3), the flow resistance in the zone above the stem (0.2 z/H) is significantly larger than that of in the stem zone. Therefore, the vertical distribution of flow velocity $z < 0.2z/H$ at location S4-1 might comply with the logarithmic distribution.

Referencing to the Kalman-Pollendel velocity distribution formula suggested by Shu et al. (2006) in Eq. (1), in this paper Eq. (2) is adopted to use depth-average velocity (U) for normalization.

$$u = u_{max} + u_* \frac{1}{k} ln\left(\frac{z}{H}\right) \tag{3.3-1}$$

$$\frac{u}{U} = a + b ln\left(\frac{z}{H}\right) \tag{3.3-2}$$

Where u is the time-averaged longitudinal velocity of a measured point, u_{max} is the maximum longitudinal velocity in a depth direction, u_* is the Shear velocity (cm/s), κ is the Von Karman's turbulence coefficient, z is the distance from the measured point to the riverbed, H is the whole water depth, U is the depth-average velocity, a= $\frac{u_{max}}{U}$ and b = $\frac{1}{k} ln\left(\frac{z}{H}\right)$ were the coefficients determined by curve fitting.

Fig. 9 shows the regressions of flow velocity for all 4 cases, which indicate that the vertical distributions of flow velocity were influenced significantly by different types of vegetation. In general, the distributions of flow velocity in the separate vertical zones appear to fit with the logarithmic distribution, but with significantly different gradients in comparison with that for P0, the bare bed without vegetation. The gradients for Cases P1 and P2 were much large in the zones above the vegetation heights, while that for P3 has a smaller velocity gradient in the stem zone, but negative gradient in the upper part of the water column where foliage is present.

From the velocity gradient, the molecular shear stress $\tau(z)$ at any level in the water column could be estimated using the following equation:

Accepted manuscript doi:
10.1680/jwama.19.00074

$$\tau(z) = \mu \frac{du}{dz} \tag{3.3-3}$$

Where τ the shear stress of a measured point, μ is is the dynamic viscosity of the fluid.

It can be anticipated that the shear stress distributions will be the same as those of velocity gradients. It is found that the maximum shear stresses at all 3 locations were between 0.12 and 0.16 cm^2/s^2, following the same patterns as shown in Fig. 10.

3.4 Turbulence kinetic energy

In order to better understand the turbulence kinetic energy generated in the test cases, TKE is calculated. The turbulence kinetic energy, which is defined as:

$$TKE = \frac{1}{2}\left(\overline{u'}^2 + \overline{v'}^2 + \overline{w'}^2\right) \tag{3.4-1}$$

where u', v' and w' were velocity fluctuations in longitudinal, transverse and vertical directions respectively.

Fig. 11 shows the distributions of TKE at 6 locations. At S1-1, the most upstream location, the TKE distributions were similar, with increased TKE level in the mid-water column. At S3-1, which is closest to the vegetated region, the TKE distributions were different, with increased levels in Cases P3 in the upper water column (z/H> 0.4). In the vegetated region (S4-1), the distribution of the TKE differs significantly in the water column, particularly for Cases P2 and P3. For Case P2, the values of TKE increase from the zone below the height of H_{P2} and reached the maximum in the zone just above the height of H_{P2}. For Case P3, due to the increased flow resistance, TKE increases from the height of H_{P3stem} (z/H= 0.2) and reaches to its maximum at the upper level above z/H= 0.4, but slightly decreases from the maximum position due to the strong flow mixing in the zone of foliage. And the maximum values of TKE for Cases P2 and P3 were more than 10 times than that of Cases P0 (Fig. 12). In the downstream region (from S6-1 to S10-1), the TKE remains increasing for Cases P2 and P3. Especially for Case P2, the TKE at locations S6-1 and S8-1 were still larger than those at S4-1 and the maximum value of TKE at location S6-1 for Cases P2 is 20 times larger than that of Cases P0 (Fig. 13), which indicates the submerged vegetation has more persisted influence on the flow turbulence than that of emergent vegetation in the downstream region.

3.5 Reynolds stress

Under the influence of the vegetation, the flow in the channel is found to be highly turbulent and strongly mixed, which will induce a high level of turbulence stress. To quantify, the analysis of Reynolds stresses is carried out. Because the main flow can be regarded as one-dimensional in longitudinal direction, the main component of Reynolds stresses would be:

$$R_{uw}/\rho = -\overline{u'w'} \quad (3.5\text{-}1)$$

which is to be presented here. Fig. 14 shows the main Reynolds stress component at 6 locations in the flume. Again, it should be noted that the different scales were used for certain sections in this Fig. for the sake of clarity. The results indicate that in the upstream region (from S1-1 to S3-1), the distributions of Reynolds stress for Cases P1, P2 and P3 were basically similar to that of Case P0, and the value of the Reynolds stress is approximately three times that of the shear stress. This indicates that the vegetation has little effect on the flow turbulence in the upstream region. In the vegetated region (S4-1), the distributions of Reynolds stress change significantly in the vertical direction because of the great influence of the vegetation. The maximum value of the Reynolds stress for Cases P2 and P3 is more than 100 times than that of the shear stress (Fig. 15). In the downstream region (from S6-1 to S10-1), the effect of vegetation on the flow turbulence remains very strong, especially in the region close to the vegetation. For Case P2, the maximum values of the Reynolds stress at locations S6-1 and S8-1 were significantly larger than that of at location S4-1. And the maximum value of the Reynolds stress at location S6-1 (for Cases P2) is more than 200 times than that of the shear stress (Fig. 16). Therefore, for the partly vegetated channel, the strong flow turbulence in the vegetated and downstream regions will make the sediment in the channel easily diffusing and make the sediment evenly distributed in the vertical direction.

3.6 Sediment concentration

As part of the experimental study, the suspended sediment concentrations were also measured, by taking the samples from the same locations of the velocity measurements. During the experiments, samples were taken twice at each measuring location by 1000 ml graduated cylinders, then filtered, dried, weighed for calculating the concentration. Malvern Mastersizer 2000 particle size analyzer was used to analyse the particle size of the sediment. The measurements, together with the velocity measurements, also enable the effect of the vegetation on the sediment transport to be investigated. According to the study of Hu and Hui (1995) on sediment concentration in natural rivers and laboratory experiments, there were 3 types of the vertical distributions of sediment concentration in an open channel as shown in Fig. 17. For Type I, the profile depends not only on the vertical pulsatile flow velocity, but also the ratio of particle size to flow depth. If the suspension index， which representes the uniformity of the vertical distribution of sediment concentration， is large and the gravity plays a dominant role, i.e. for the coarse sands, the profile would be Type. If the suspension index is small and the turbulent diffusion plays a dominant role, the profile would be Type III.

Fig. 18 shows the distributions of the sediment concentration profiles at 3 locations S1-1, S4-1 and S8-1. It is clear that the profiles in the upstream region (S1-1) generally were of both Types I and II as defined in Fig. 17a, indicating that the flow turbulence is weak in the upstream, and the gravity of sediment plays a dominant role in sediment transport. In the vegetated region (S4-1), due to the influence of vegetation, the distribution of the sediment

Accepted manuscript doi:
10.1680/jwama.19.00074

concentration changes greatly in comparison with that in the upstream region. The sediment concentrations for Cases P2 and P3 decrease significantly and their distributions were of Type III, which indicates that the turbulent diffusion plays a dominant role in sediment transport. In the downstream region (S8-1), the vertical distribution of sediment concentration for Cases P2 and P3 becomes smaller and very uniform. There could be two possible reasons: 1) Influenced by the decreased velocity, the coarse sediments (D50 > 0.1mm) were mostly deposited in the upstream and vegetated region, and fine sediments (D50<= 0.1mm) were still remained in suspension; 2) For Cases P2 and P3, the turbulent diffusion of the flow in the downstream region is significantly stronger than that of Cases P0 and P1, which will be beneficial to the diffusion of suspended sediment in the flow.

From the experiments, it is found that the fine sediment concentration hardly changes in the water column for Cases P0, P1, P2 and P3, while, the coarse sediment concentration decreases. The differences indicate that the fine sediment suspension is independent of the types of vegetation and/or their locations in the channel, while the coarse sediments trend to deposit. Fig. 19 shows the vertical distributions of concentration for sediments with different sizes for all 4 cases. In this figure, the coarse sediment concentrations for Cases P2 and P3 were found to decrease rapidly in the region from S1-1 to S4-1, but to be almost constant in the region from S4-1 to S8-1. This may be attributed to the sudden increase of flow resistance in the local region (from S3-1 to S4-1) and strong flow turbulence intensity in the other region (from S4-1 to S8-1).

3.7 Sediment transport rate

One of the important objectives in the present study is to investigate the relationship between the flow structures and sediment transport in the vegetated channel. Therefore, the sediment transport rates were calculated from the measured flow velocity and sediment concentration. The sediment transport rate is defined as:

$$S = \overline{C} \cdot \overline{U} \tag{3.7-1}$$

Where $\overline{C}$ was the cross-sectional averaged sediment concentration, $\overline{U}$ was the cross-sectional averaged velocity. As shown in Fig. 20, in the upstream region (S1-1), the distributions of the sediment transport rate for Cases P1, P2 and P3 were found to be mostly similar to that of Case P0. This indicates that the vegetation has little effect on the sediment transport rate in the upstream region. In the vegetated region (S4-1), the distribution of the sediment transport rate for Case P1 is still similar to that of Case P0, whilst, the distributions for Cases P2 and P3 change significantly in the vertical direction. For Case P2, the sediment transport rate in the zone below the height of 0.2 z/H is close to zero. In contrast, for Case P3, the sediment transport rate in the zone below the height of 0.2 z/H is very large, while the sediment transport rate in the zone above height of 0.5 z/H level is close to zero. In the downstream region (S8-1), the distributions of the sediment transport rate under Cases P1 and P3 were similar to that of Case P0, whilst, for Case P2, the vertical distribution of the

sediment transport rate is rather uniform. The reason might be the strong flow turbulence intensity affecting sediment transport rate.

Fig. 21 shows the rates of sediment transport for Cases P0, P1, P2 and P3 along the channel. As shown in the figure, the rates of sediment transport for Cases P0, P1, P2 and P3 are nearly the same in the upstream region. Whilst, in the vegetated region, for Cases P0 and P1, the rates are decreased slightly, but for Cases P2 and P3, the rates are decreased significantly. In the downstream region, for Cases P0 and P1, the rates are still decreased slightly, while, the rate was basically constant for Cases P2 and P3.

The sediment deposition for the all cases was recorded by the photos taken during the experiments. Fig. 22 shows the sediment deposition in the flume for all 4 cases. For Cases P0 and P1, the sediment deposition was small, seen as a thin layer on the bed over the entire length of the flume. This means that the sediment retention by the small sized vegetation, P1, was small where most the sediments are transported to the downstream. However, for Cases P2 and P3, a large amount of sediment deposition was found at the upstream head of the vegetated region. For large vegetation, the submerged vegetation has a greater impact on sediment transport than that of emergent vegetation.

4 Conclusions

Understanding of effect of vegetation on the flow and sediment transport was highly important for modern river management and water ecological restoration. This study investigates the effect of submerged and emergent vegetation on 3D flow structures and sediment transport in a flume. Based on the achievement, the following conclusions can be drawn. (1) The existing of vegetation generates a great resistance to flow, which significantly alters the vertical distributions of velocity, especially in the vegetated and downstream regions. For submerged and emergent vegetation in the vegetated region, the velocity can be categorized into two and three regions, respectively. At S9-1, the velocity distributions are mostly recovered except for emergent vegetation, which was seen to be almost fully recovered at S10-1. (2) In comparison with the non-vegetated case, the turbulence kinetic energy and the Reynolds stresses in the vegetated and downstream regions are much higher, with the maximum values of turbulence kinetic energy are in excess of 10 and 20 times larger, while the maximum values of Reynolds stresses are in excess of 100 and 200 times larger, indicating strong flow turbulence and momentum exchange in these two regions. (3) For submerged vegetation, the sediment transport of the vegetated region mainly occurs in the zone above the height of vegetation, while for the emergent vegetation, the transport was mainly concentrated in the stem zone. Meanwhile, the fine sediment suspension was independent of the types of vegetation. The increased resistance by vegetation causes the coarser suspended sediment concentration to decrease along the channel. (4) For small sized vegetation, the sediment deposition was small, seen as a thin layer on the bed over the entire length of the flume. This means that the sediment retention by the small-sized vegetation was insignificant. But for large vegetation, the significant sediment deposition was found at the

upstream head of the vegetated region, especially, the submerged vegetation has a greater impact on sediment transport than that of emergent vegetation.

Acknowledgements

The paper was mainly written in Cardiff University. The authors would like to express their gratitude to Cardiff University for its comprehensive supports. The authors thank Professor Yonghui Zhu and PhD student Dong Chen for their help in carrying out the experiments. and the staff of Changjiang River Scientific Research Institute for technical assistance. The authors appreciated the comments of the editors and reviewers which helped to improve this article.

Funding

This work was partly supported by National Key R&D Program of China [grant 2016YFC0402310, 2016YFC0402105], and National Natural Science Foundation of China [grant 51679011, 51309022, 51579172, 51609016].

Notation

A_{ve} = accumulative areas (cm^2);

C= Sediment volume concentration (-);

CV= Sediment transport rate(-);

d_{50}= Median diameter of experimental sand (mm);

F= Froude number;

H= whole water depth (cm);

H_0= the water depth at the outlet of the flume (cm);

H_1= the water depth at the upstream of the vegetated region (cm);

H_2= the water depth at the head of the vegetated region (cm);

H_3= the water depth at the tail of the vegetated region (cm);

H_{P1}=the height of vegetation P1 (cm);

H_{P2}= the height of vegetation P2 (cm);

H_{P3}= the height of vegetation P3 (cm);

H_{P3stem}= the height of stem for vegetation P3 (cm);

h_{ve}= vegetation with its height (cm);

J= surface slope (-);

R_e= Reynolds number (-);

Accepted manuscript doi:
10.1680/jwama.19.00074

R_{uw}= the Reynolds stress tensor (g cm s^{-2});

S_0 = bed slope;

S_s = water surface slope;

TKE= turbulence kinetic energy (cm^2 s^{-2});

u= time-averaged longitudinal velocity of a measured point (cm s^{-1});

u_{max}= maximum longitudinal velocity in a depth direction (cm s^{-1});

u_*=Shear velocity (cm s^{-1});

$-\overline{u'w'}$=Reynolds stress in vertical direction on plane perpendicular to longitudinal direction (cm^2 s^{-2});

U= time-averaged longitudinal velocity of a measured point (cm s^{-1});

X= Longitudinal direction (-);

Y= Transverse direction (-);

Z=Vertical direction (-);

z= the distance from the measured point to the riverbed (cm);

κ= Von Karman's turbulence coefficient;

ρ= Fluid density (g cm^{-3});

τ= shear stress (g cm s^{-2})

References

Carollo, F. G., Ferro, V., & Termini D. (2002). Flow velocity measurements in vegetated channels. Journal of Hydraulic Engineering, 128, 664-673.

Changjiang River Scientific Research Institute. (2005, March). The study on model sediment experiment in Changjiang River flood control model (CRSRI/2005-132). Wuhan, China: Sun, G., & Wei, G.

Changjiang River Water Resources Commission Hydrology Bureau (2016, October). The compilation of measurement results about research on the fluvial process in the meandering reach of the downstream Yangtze River after impounding of the Three Gorges Project (CRSRI/2016-204). Wuhan, China: Zhou, F., & Tao, W.

Elliott, A. (2000). Settling of fine sediment in a channel with emergent vegetation. Journal of Hydraulic Engineering, 126, 570-577.

Fagherazzi, S., Bryan, K. R., & Nardin, W. (2017). Buried alive or washed away: The challenging life of mangroves in the mekong delta. Oceanography, 30(3), 48–59.

Ghisalberti, M., Nepf, H. (2002). Mixing layers and coherent structures in vegetated aquatic flow. J. Geophys. Res. 107(C2), doi: 10.1029/2001JC000871.

Ghisalberti, M., Nepf, H. (2004). The limited growth of vegetated shear-layers. Water Resour. Res. 40, W07502, doi:10.1029/2003WR002776.

Ghisalberti M, Nepf H. (2006). The structure of the shear layer over rigid and flexible canopies. Environ. Fluid Mech. 6:277–301.

Graf ,W. H., & Yulistiyanto, B. (1998). Experiments on flow around a cylinder; the velocity and vorticity fields. Journal of Hydraulic Research, 34, 637-653.

Hu, C., & Hui Y. (1995). Mechanisms and statistical laws of flow and sediment movement in open channel. Beijing, China: Science Press.

Li, Y., Du, Wei., & Yu, Z. (2015). Impact of flexible emergent vegetation on the flow turbulence and kinetic energy characteristics in a flume experiment. Journal of Hydro-environment Research, 9, 354-367.

Lu, S. (2008). Experimental Study on Suspended Sediment Distribution in Flow with Rigid Vegetation. Hohai University, Nanjing, China.

Mars, M., Kuruvilla, M., Goen, H. (1999). The role of submergent macrophyte triglochin huegelii in domestic greywater treatment. Ecol. Eng. 12, 57–66.

Nezu, I., & Onitsuka, Kouki. (2001). Turbulent structures in partly vegetated open-channel flows with LDA and PIV measurements. Journal of Hydraulic Research, 39, 629-642.

Ikeda, S., & Kanazawa, M. (1996). Three-Dimensional Organized Vortices above Flexible Water Plants. Journal of Hydraulic Engineering, 122, 634-640.

Jordanova, A.A., & James, C.S. (2003). Experimental Study of Bed Load Transport through Emergent Vegetation. Journal of Hydraulic Engineering, 129, 474-478.

Nepf, H. M. (1999). Drag, turbulence, and diffusion in flow through emergent vegetation. Water Resour. Res. 35, 479–489.

Nepf, H. M., Vivoni, E. (2000). Flow structure in depth-limited, vegetated flow. J. Geophys. Res. 105(28), 547–557.

Nepf, H., Ghisalberti, M., White, B., Murphy, E. (2007). Retention time and dispersion associated with submerged aquatic canopies. Water Resour. Res. 43, W04422, doi:10.1029/2006WR005362.

Nepf, H. M. & Ghisalberti, M. (2008). Flow and transport in channels with submerged vegetation. Acta Geophysica, 56(3), 753-777.

Nepf, H. M. & Heidi, M. (2012a). Flow and transport in regions with aquatic vegetation. Annual Review of Fluid Mechanics, 44(1), 123-142.

Nepf, H. M. (2012b). Hydrodynamics of vegetated channels. Journal of Hydraulic Research, 50(3), 262-279.

Ni, J., Wang, G., & Zhang H. (1991). The theory of sediment and flow transport and the newest applications. Beijing, China: Science Press.

Okamoto, T., & Nezu, I. (2010). Flow resistance law in open-channel flows with rigid and flexible vegetation. In Dittrich, Koll, Aberle & Geisenhainer (Eds), River Flow 2010. Proceedings of the International Conference on Fluvial Hydraulics(pp.261-268), Braunschweig, Germany.

Pollen, N., Simon, A. (2005). Estimating the mechanical effects of riparian vegetation on stream bank stability using a fiber bundle model. Water Resour. Res. 41, W07025, doi:10.1029/2004WR003801.

Qian, N., & WAN, Z. (1986). Sediment movement mechanics. Beijing, China: Science Press.

Qu, G. (2014). Experimental Study on Water and Sediment Transport in Open Channel Flow with Vegetation. Wuhan University, Wuhan, China.

Qu, G., Zhang, X., & Chen, D. (2015). Experimental study on flow resistance characteristics in open channel with flexible vegetation. Journal of Hydraulic Engineering, 11, 1344-1351.

Righetti, M. (2008). Flow analysis in a channel with flexible vegetation using double-averaging method. Acta Geophysica, 56(3), 801-823.

Shi, B., & Cao, S. (2000). The Control Sand Dynamics Using Vegetation. Qingdao, China: Ocean University of China Press.

Shu, A., Liu Q., & Fei, X. (2006). Unified laws of velocity distribution for sediment laden flow with high and low concentration. Journal of Hydraulic Engineering, 37, 1175-1180.

Stephan, U., & Gutknecht, D. (2002). Hydraulic resistance of submerged flexible vegetation. Journal of Hydrology, 269, 27-43.

Su, X., & Li, C. (2002). Large eddy simulation of free surface turbulent flow in partly vegetated open channels. The International Journal for Numerical Methods in Fluids, 39, 919-937.

Tang, H., Yan, J., & Lu, S. (2007). Advances in research on flows with vegetation in river management. Journal of China Institute of Water Resources and Hydropower Research, 18, 785-792.

Termini, D. (2015). Flexible vegetation behavior and effects on flow conveyance: experimental observations. Int. J. River Basin Manage. 13 (4), 401–411.

Termini, & Donatella. (2017). Vegetation effects on cross-sectional flow in a large amplitude meandering bend. Journal of Hydraulic Research, 1-7.

Ursula, S., & Dieter, G. (2002). Hydraulic resistance of submerged flexible vegetation. Journal of Hydrology, 269, 27-43.

Wang, X., Shao, X., & Li D. (2002). The Basis of River Dynamics. Beijing, China: China Water and Power Press.

Wang, Z. Y., Lee, J. H. W., Melching, C. S. (2014). River dynamics and integrated river management. Berlin and Beijing: Springer Verlag and Tsinghua Press.

Weston, N. B. (2014). Declining sediments and rising seas: An unfortunate convergence for tidal wetlands. Estuaries and Coasts, 37(1), 1–23.

Wilson, C., Stoesser, T., & Pinzen, B. (2003). Open channel flow through different forms of submerged flexible vegetation. Journal of Hydraulic Engineering, 129, 847-853.

Yang, J. Q., & Nepf, H. M. (2018). A turbulence-based bed-load transport model for bare and vegetated channels. Geophysical Research Letters, 45, 10428–10436. https://doi.org/10.1029/2018GL079319

Yang, Q. J., & Nepf, H. M. (2019). Impact of vegetation on bed load transport rate and bedform characteristics. Water Resources Research, 55. https://doi.org/10.1029/2018WR024404

Yoon, B., & Ettema, R. (1993). Droplet trajectories and icing-collision efficiencies for cylinders determined using LDV. Cold Regions Science and Technology, 21, 381-397.

Zhou, F., & Tao, W. (2016). The compilation of measurement results about research on the fluvial process in the meandering reach of the downstream Yangtze River after impounding of the Three Gorges Project. Changjiang River Water Resources Commission Hydrology Bureau, Wuhan, China.

Table 1 The hydraulic conditions measured in the vegetated region

Case	Vegetation Type	Q (L/s)	U (cm/s)	S_0 (1/1000)
P0	None	30	17.15	0.18
P1	P1	30	17.16	0.30
P2	P2	30	17.23	0.97
P3	P3	30	17.31	5.00

Figure captions

Fig. 1. Experimental setup showing the artificial vegetation

Fig. 2 Schematic diagram of the experimental flume: (a) Side view; (b) Top view (not to scale)

Fig. 3. Three types of artificial vegetation

Fig. 4 Types of the vegetation and the cumulative area against the height

Fig. 5 Grading curves of sediment used

Fig. 6 Vertical profiles of normalized longitudinal velocity (u/U) at stream-wise locations (dotted and dashed lines indicating the heights of the vegetation P1, P2, and the stem part of P3)

Fig. 7 Vertical profiles of normalized longitudinal velocity (u/U) at transverse locations

Fig. 8 Distributions of the flow velocity gradients at S1, S4 and S8 locations

Accepted manuscript doi:
10.1680/jwama.19.00074

fig1

Accepted manuscript doi:
10.1680/jwama.19.00074

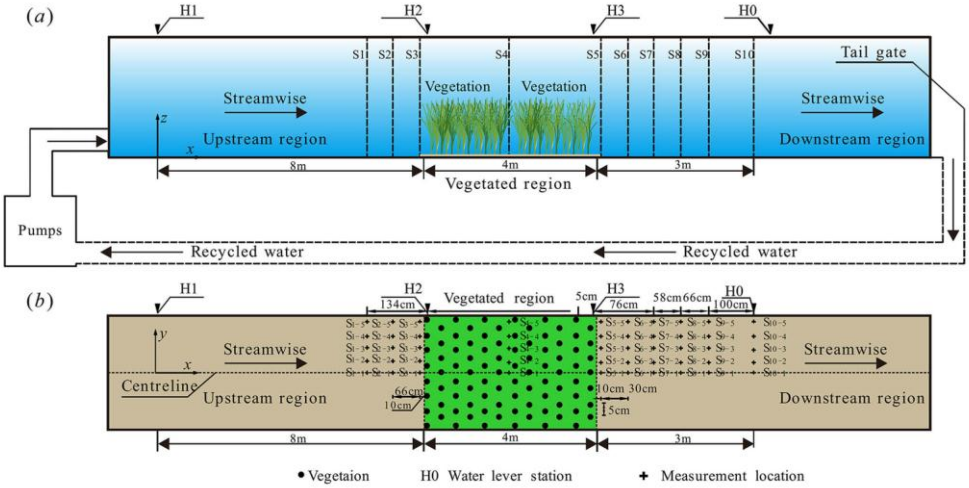

fig2

未命名 -3

Accepted manuscript doi:
10.1680/jwama.19.00074

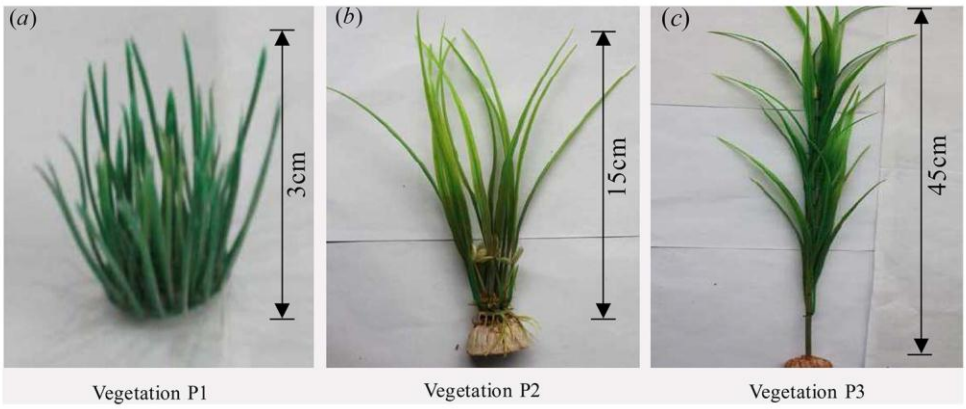

fig3

Accepted manuscript doi:
10.1680/jwama.19.00074

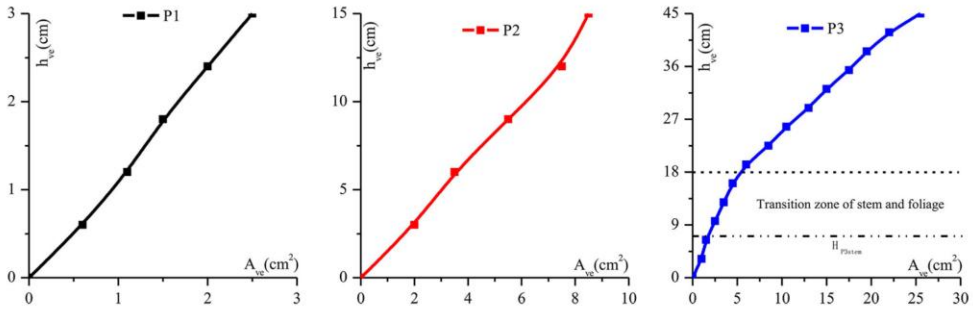

fig4

Accepted manuscript doi:
10.1680/jwama.19.00074

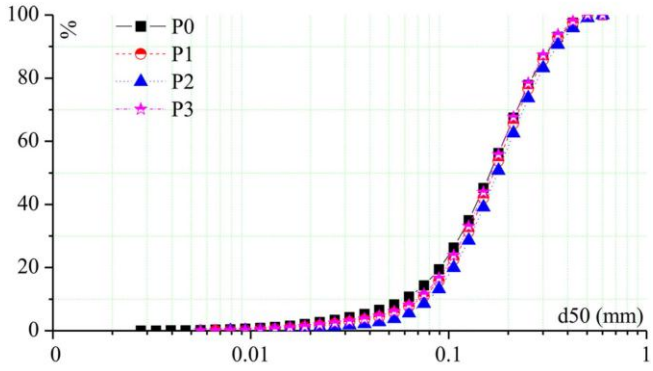

fig5

Accepted manuscript doi:
10.1680/jwama.19.00074

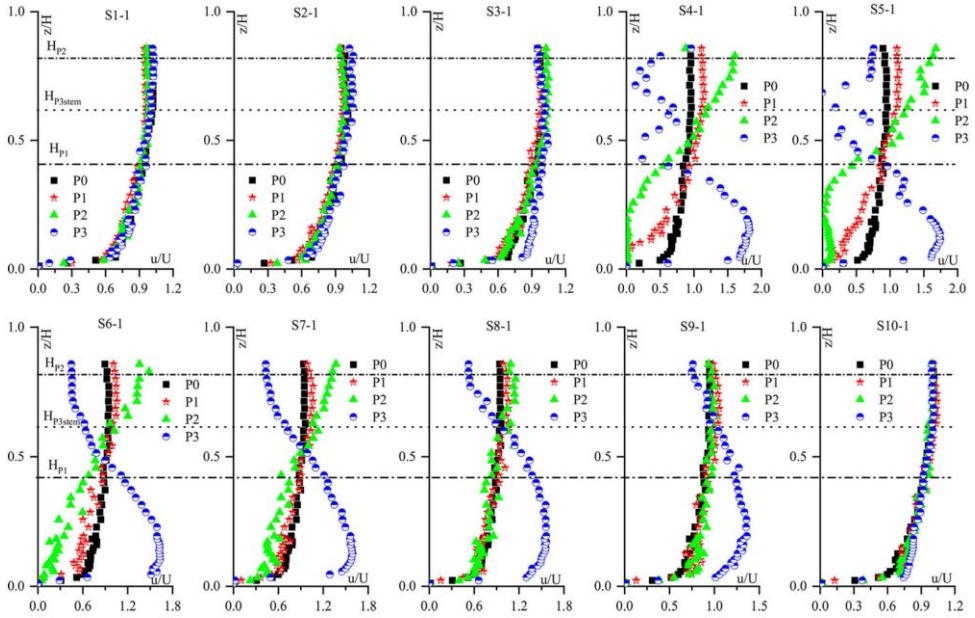

fig6

Accepted manuscript doi:
10.1680/jwama.19.00074

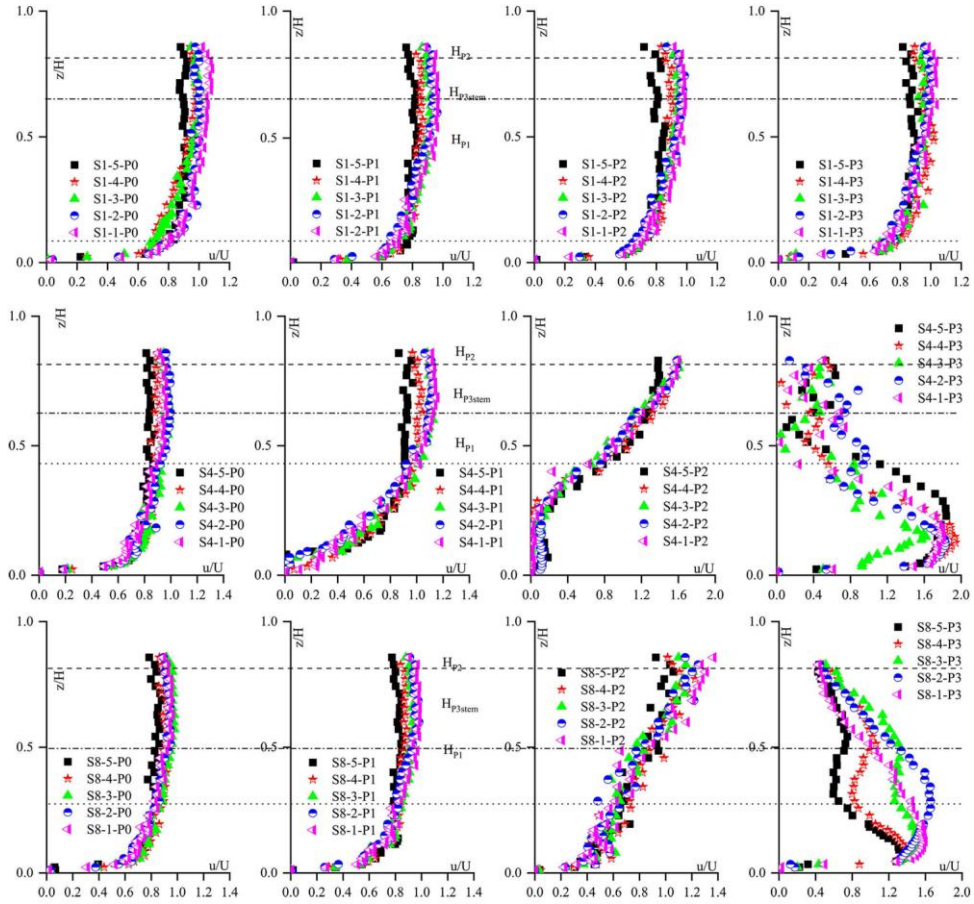

fig7

Accepted manuscript doi:
10.1680/jwama.19.00074

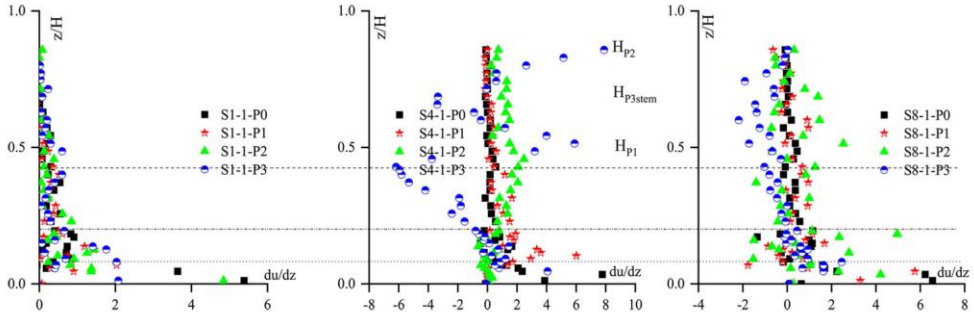

fig8

Accepted manuscript doi:
10.1680/jwama.19.00074

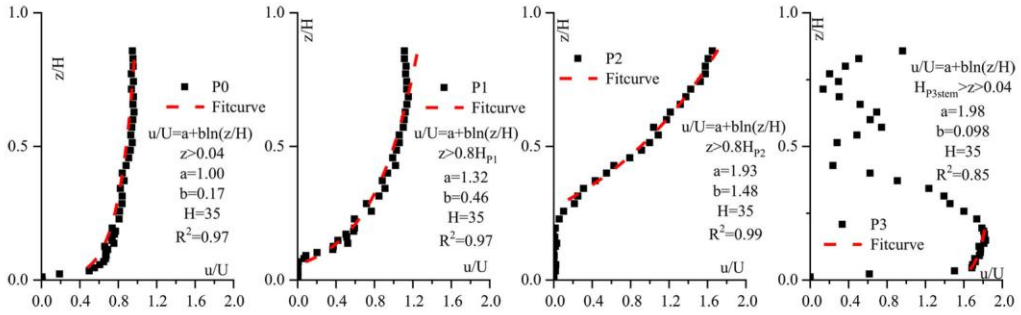

fig9

Accepted manuscript doi:
10.1680/jwama.19.00074

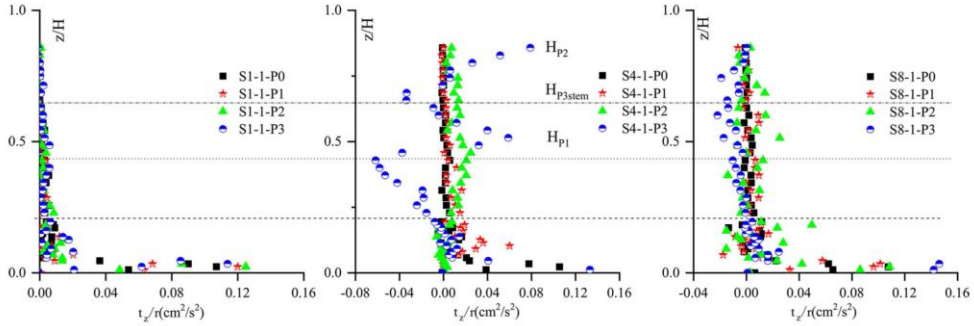

fig10

Accepted manuscript doi:
10.1680/jwama.19.00074

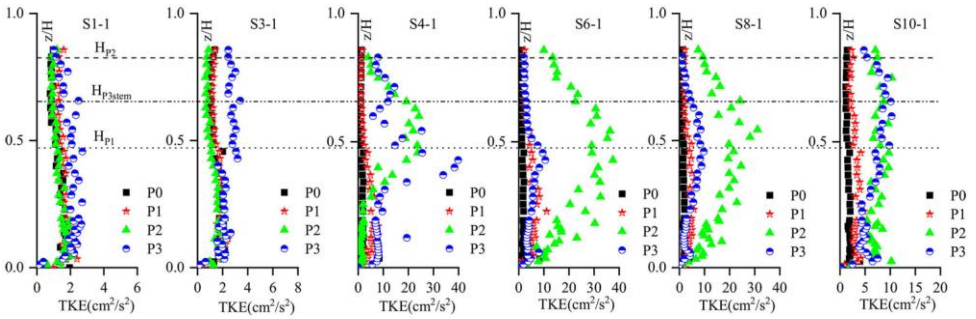

fig11

Accepted manuscript doi:
10.1680/jwama.19.00074

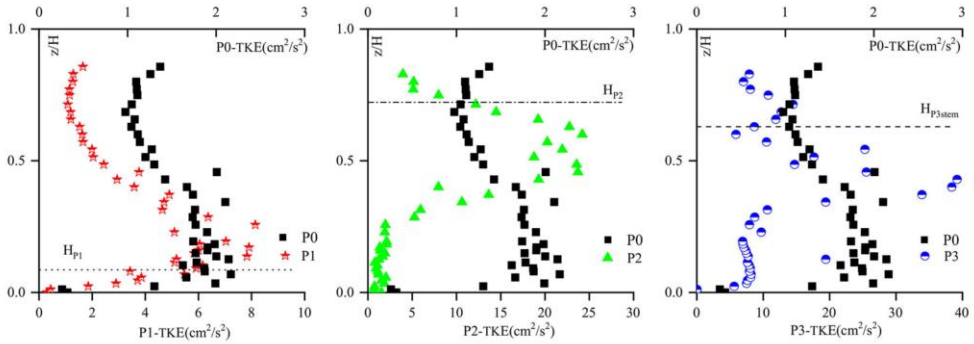

fig12

Accepted manuscript doi:
10.1680/jwama.19.00074

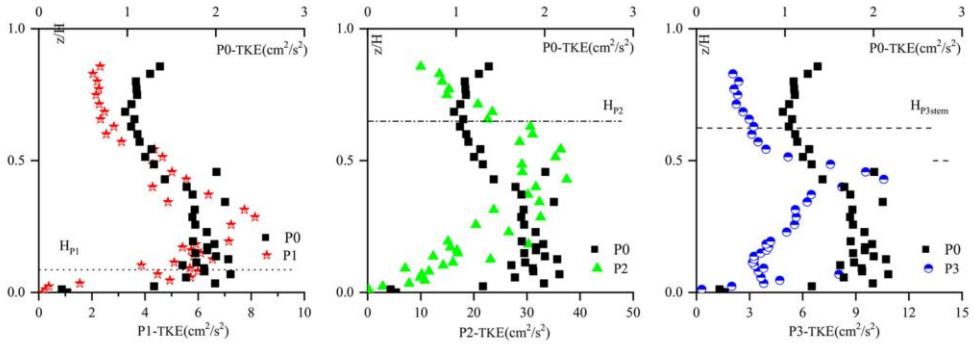

fig13

Accepted manuscript doi:
10.1680/jwama.19.00074

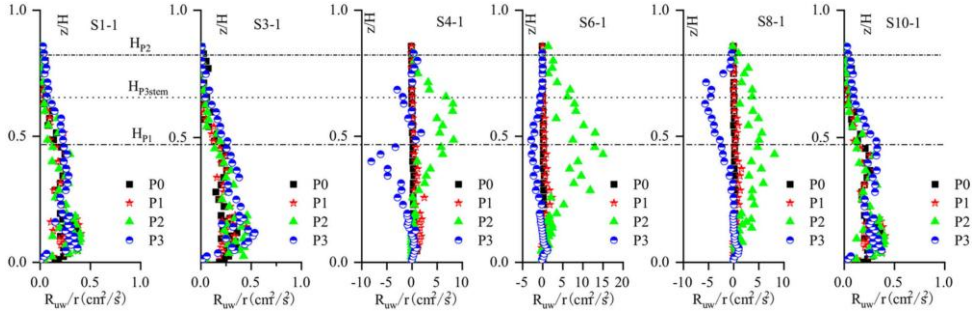

fig14

Accepted manuscript doi:
10.1680/jwama.19.00074

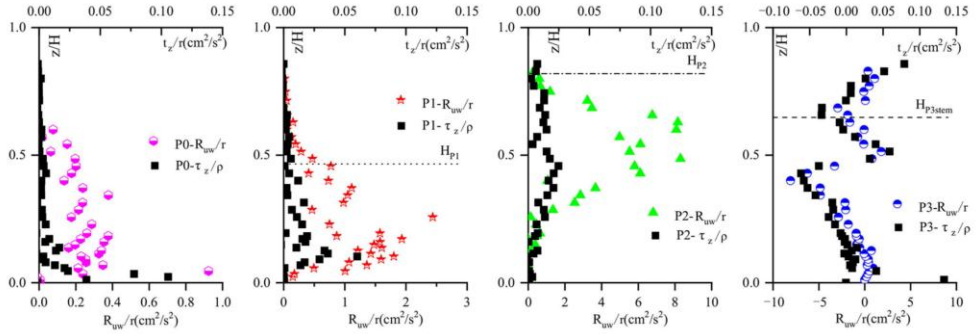

fig15

Accepted manuscript doi:
10.1680/jwama.19.00074

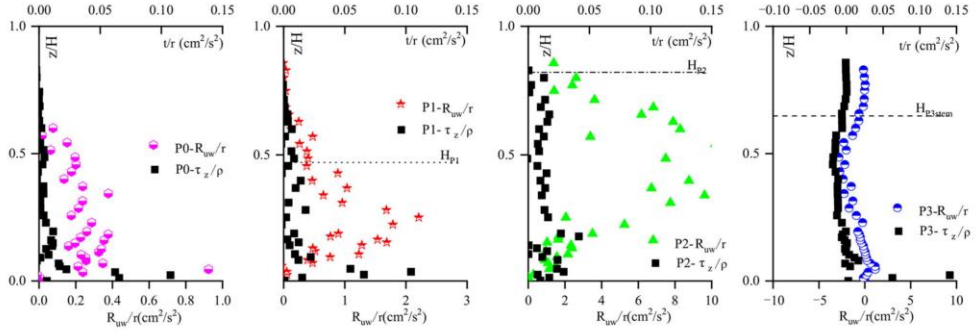

fig16

Accepted manuscript doi:
10.1680/jwama.19.00074

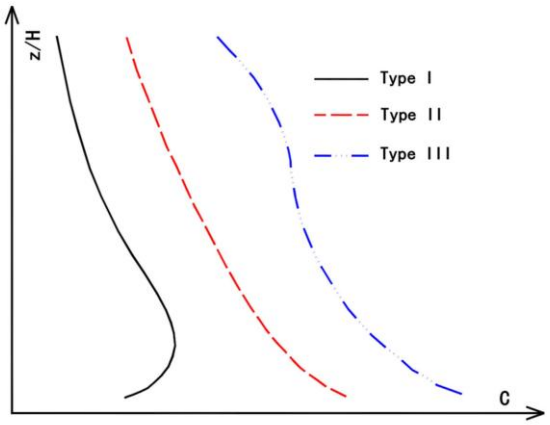

fig17

Accepted manuscript doi:
10.1680/jwama.19.00074

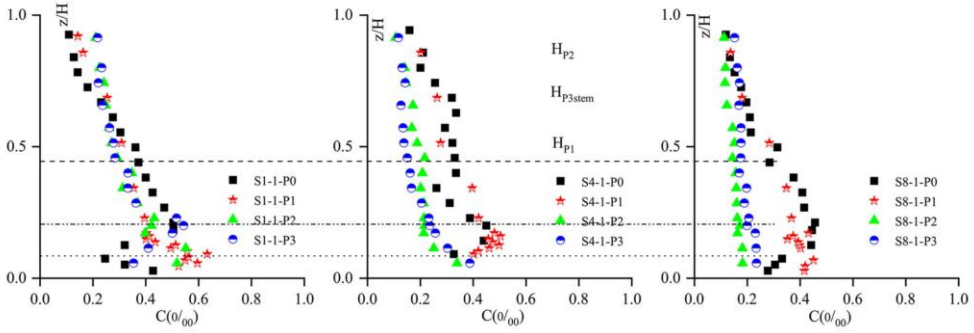

fig18

Accepted manuscript doi:
10.1680/jwama.19.00074

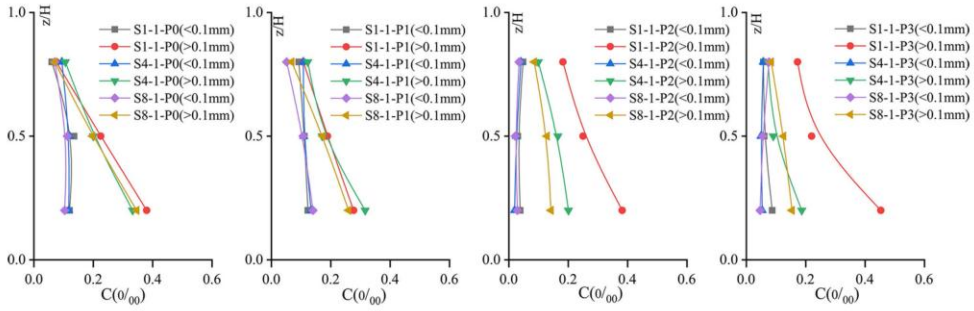

fig19

Accepted manuscript doi:
10.1680/jwama.19.00074

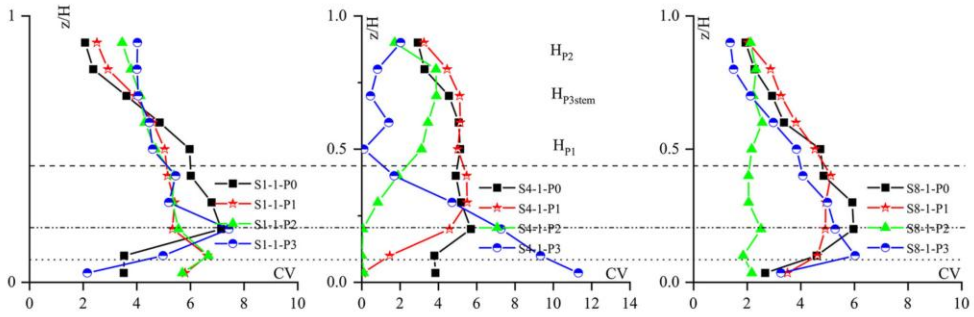

fig20

Accepted manuscript doi:
10.1680/jwama.19.00074

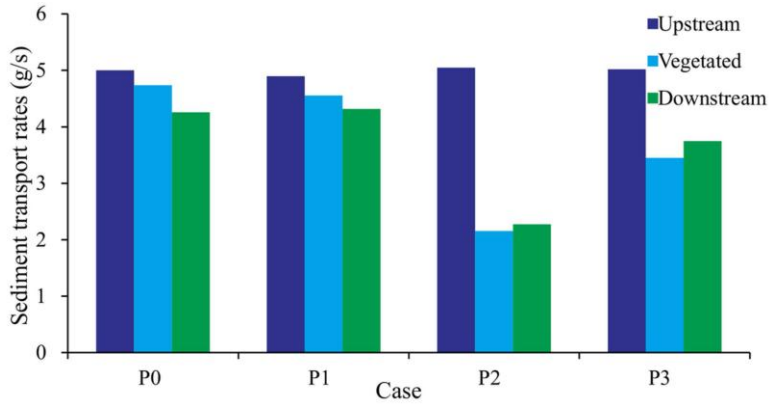

fig21

Accepted manuscript doi:
10.1680/jwama.19.00074

fig22